UDK 621.039.568:669.14.018:539.42
Professional article/Strokovni članek

ISSN 1580-2949
MTAEC9, 44(4)227(2010)

INFLUENCE OF δ-FERRITE ON THE FATIGUE RESISTANCE OF BLADE MATERIALS

VPLIV δ-FERITA NA UTRUJENOSTNO TRDNOST JEKEL ZA LOPATICE

Pavlína Hájková[1], Jiří Janovec[1], Jan Siegl[2], Bohumil Smola[3], Michaela Vyroubalová[1], Daniela Tůmová[1]

[1]CTU in Prague – Faculty of Mechanical Engineering, Karlovo nám. 13, 121 35 Praha 2, Czech Republic
[2]CTU in Prague – Faculty of Nuclear Sciences and Physical Engineering, Trojanova 13, 121 35 Praha 2, Czech Republic
[3]Charles University in Prague – Faculty of Mathematics and Physics, KE Karlovu 5, 121 35 Praha 2, Czech Republic
pavlina.hajkova@fs.evut.cz

Prejem rokopisa – received: 2009-11-16; sprejem za objavo – accepted for publication: 2010-02-21

The low-pressure parts of a TG 1000 MW turbine, for the third wheels, are made from modified 12 % Cr martensitic steel AK1 TD.9, and the fourth, are made from X2CrNiMo13-4 steel. The fracture of the third turbine wheel at the point of the connection part of the blade has a high-cycle fatigue character with multiple initiation sites. An analysis of the microstructure has proved the influence of both the δ-ferrite content and the arrangement on the initiation point of the fatigue process. Also, an inspection of the fatigue crack's kinetics in relationship to the operating mode of the power plant has been carried out.

Key words: low-pressure turbine, steel, fatigue fracture, microstructure, δ ferrite

Nizkotlačni deli turbine TG 1000 MW iz tretjega venca so iz modificiranega 12-odstotnega Cr martenzitnega jekla AK TF.9, iz četrtega venca pa iz jekla X2CrNiMo 13-4. Prelom tretjega turbinskega venca v točki vpetja ima značaj visoke ciklične utrujenosti z mnogimi začetnimi mesti. Analiza mikrostrukture je pokazala vpliv vsebine in porazdelitve δ-ferita na začetno točko procesa utrujenosti. Ugotovljena je bila tudi povezava kinetike utrujenostne razpoke z načinom dela turbine.

Ključne besede: nizkotlačna turbina, jeklo, utrujenostna razpoka, mikrostruktura, δ-ferit

1 INTRODUCTION

In October 2008 the blade of the third turbine wheel (3TW) placed on the third low-pressure part (3LP) of the TG1 broke. Consequently, the broken blade damaged the turbine wheels numbers 3 and 4 on the LP1, LP2 and LP3 (see **Figure 1**). The break in the blade occurred near the connection part (**Figure 2**) during the blade's operation. Cracks in the connection-part regions within the turbine wheels of other low-pressure parts were discovered with defectoscopic analysis. The damaged connection part is shown in **Figure 2**. The chemical composition, mechanical properties, fractography and time-dependent estimation of the crack propagation of the removed blades were tested. The scheme of the damaged blades within the whole turbine vessel is shown in **Figure 3**.

2 EXPERIMENTAL PROCEDURE

2.1 Materials

The investigated blades (see **Table 1**) were drop forged, and a new steel, 1.4939, was investigated as a possible substitute material for the 3.TW.

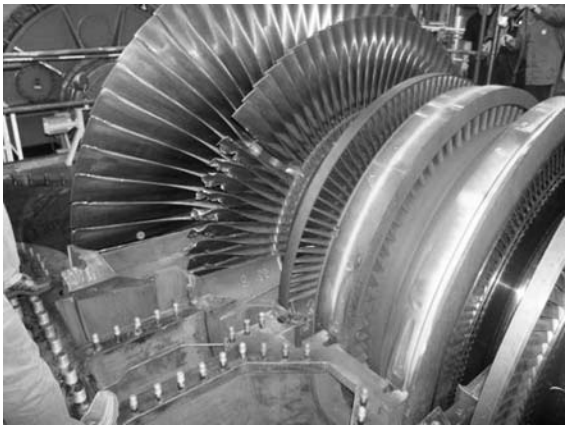

Figure 1: Damage to the 3TW on the TG1
Slika 1: Poškodba 3TW na TG 1

Figure 2: Damage to the connection part
Slika 2: Poškodba na mestu vpetja

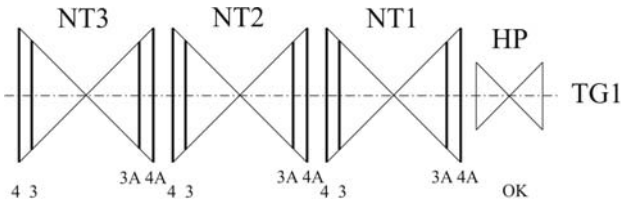

Low-pressure part	Turbine Wheel number	Blade number
3LP	3. TW	152, 156, 106
1LP	4. TW	344
3LP	3. TW (suggestion)	1.4939

Figure 3: Scheme of broken blades within the whole turbine vessel
Slika 3: Shema prelomljenih lopatic v turbinskem ohišju

Table 1: Investigated samples
Tabela 1: Vzorci za preiskave

Blade No.	Low-pressure part	State	Material
152	3NT	Destroyed	modified 12 % Cr martensitic steel AK1 TD.9
156	3NT	Laboratory broken	modified 12 % Cr martensitic steel AK1 TD.9
106	3NT	Additionally identified	modified 12 % Cr martensitic steel AK1 TD.9
New material 1.4939		Identified	1.4939 + QT
344	NT 4a	OK	X2CrNiMo13-4 steel (WEV 400)

2.2 Investigation methods

2.2.1 Evaluation of the chemical and microchemical composition of the turbine-blade material

Three different devices were used for the chemical analysis: a ARL 34600 OE quantimeter, a Belec Vario Lab spectrometer, and an Electron Microanalysis Camebax MICRO CAMECA with a KAVEX energy-dispersion analyzer. These various devices were used because of the great variability in the chemical composition within the different melts.

2.2.2 Verification of the mechanical properties of the turbine blades

The mechanical properties were determined with tensile, Charpy impact and Brinell hardness tests. Two different types of samples with respect to the turbine-blade orientation were extracted. The first were extracted from the connection part perpendicular (PN) to the blade axis, the second samples extracted from the blade base in a parallel orientation (PO) to the blade axis.

Tensile tests were carried out on an INSTRON 100kN Series IX Automated Materials Testing System according to the testing conditions of the standard ČSN EN 10002-1. A Padostroj Charpy 300 J was used for the Charpy impact tests, according to the standard (with a test temperature of 20 °C and specimen dimensions of (10 × 10 × 55) mm with the V-notch) ČSN EN 10045-1. The Brinell hardness was determined with an EMCO-TEST M4C universal hardness tester according to the standard ČSN EN 6506-1.

2.2.3 Light-microscopy examination of metallographic samples

Qualitative and quantitative microstructural analyses of the base material and of the fracture areas were carried out for the perpendicular (PN) and parallel (PO) samples cut out from the blades. The samples were taken from the fracture zone and from the middle parts of the blade bodies. For the examination a Zeiss-Neophot 32 light microscope with suitable magnifications was used. For the X2CrNiMo13-4 steel, a solution of 5 mL HCl, 1 mL TNP (2,4,6-trinitrofenol) and 95ml of ethyl alcohol was used as an etching agent. The 12% Cr martensitic steel AK1 TD. 9 was etched in a water solution with 2.5 mL of HNO_3.

2.2.4 Electron-microscopy examination of metallographic samples

The samples for examination with transmission electron microscopy were prepared with spark erosion and cut parallel to the crack-propagation plane. From the thin plates, discs of 2.7 mm in diameter were prepared with spark-erosion cutting and mechanically thinned to 70–80 μm. Thin foils for the electron-microscopy observation were prepared with electrolytic polishing in TENUPOL equipment, applying a 6 % solution of $HClO_4$ in methanol, a temperature of 35 °C and a current of 150 mA. The samples were examined in a JEOL JEM2000FX transmission electron microscope and the energy-dispersion microanalyzer of an RTG emission LINK AN10000 was used for the chemical analyses.

3 RESULTS AND DISCUSSION

3.1 Chemical composition and mechanical properties

The results of the chemical analysis and the measurements of the mechanical properties (yield strength, ultimate strength, ductility, reduction of cross-section area, Charpy impact strength, hardness) are summarized in **Table 2**, **Table 3** and **Table 4**. It is evident that the requirements of the standards AK1 TD.9 and WEV 400 are fulfilled almost completely. Only the lower Charpy impact strength was determined for the material of the blades 152, 156, 106. This can be due to the operation of the components for a long time or the non-standard operating conditions.

3.2 Optical microscopy

The microstructure of the base material was typical for modified 12 % Cr martensitic steel. The microstructure of the heat-treated (quenched and annealed) steel is shown in **Figure 4**. The large amount of δ-ferrite present in the microstructure was aligned in rows, oriented parallel with the initial crack growth and may have

Table 2: Chemical composition (*w*/%)
Tabela 2: Kemična sestava jekel (*w*/%)

Sample	C	Si	Mn	P	S	Cr	Ni	Mo	V	W
Specification AK1 TD.9	0.10–0.16	< 0.60	0.60	< 0.025	< 0.015	10.5–12	1.5–1.8	0.35–0.5	0.18–0.30	1.6–2.0
152	0.142 ±0.004	0.371 ±0.002	0.46 ±0.004	0.022 ±0.002	0.01 ±0.001	11.71 ±0.14	1.853 ±0.022	0.448 ±0.004	0.3 ±0.006	1.77 ±0.142
156	0.143 ±0.002	0.374 ±0.002	0.462 ±0.004	0.021 ±0.002	0.011 ±0.002	11.62 ±0.022	1.843 ±0.012	0.451 ±0.006	0.302 ± 0.006	1.768 ±0.044
106	0.16 ±0.004	0.31 ±0.006	0.41 ±0.006	0.024 ±0.004	0.010 ±0.002	11.44 ±0.014	1.90 ±0.042	0.44 ±0.004	0.29 ±0.008	1.59 ±0.022
Specification 1.4939	0.15	< 0.35	0.9	0.020	0.015	12.50	3.00	2.00	0.40	–
New mat. 1.4939+QT	0.314 ±0.004	0.102 ±0.004	0.829 ±0.018	0.011 ±0.002	0.007 ±0.001	11.57 ±0.20	2.498 ±0.076	1.568 ±0.014	0.345 ±0.008	0.222 ±0.036
Specification WEV 400	max. 0.05	0.15–0.35	0.20–0.80	max. 0.020	max. 0.025	12.0–14.0	3.5–4.5	0.30–0.50	–	–
344	0.013 ±0.002	0.29 ±0.002	0.76 ±0.004	0.015 ±0.008	0.002 ±0.001	12.88 ±0.012	4.14 ±0.022	0.46 ±0.003	0.02 ±0.002	0.017 ±0.014

Table 3: Mechanical properties
Tabela 3: Mehanske lastnosti

Sample (blade No.)	Yield Strength $R_{p\,0.2}$/MPa	Ultimate strength R_m/MPa	Ductility *A*/%	Contraction *Z*/%
152/1 PN	845	957	20.0	55.4
152/2 PN	860	969	20.0	55.4
156/1 PO	830	948	18.3	55.4
156/2 PO	835	966	16.7	55.4
156/3 PN	820	962	16.7	55.4
106/1 PO	860	965	16.7	50.9
106/2 PO	849	957	17.3	55.4
106/3 PN	865	976	16.7	50.9
344/1 PO	951	989	18.3	81.2
344/2 PO	950	984	18.0	79.7
344/3 PN	952	987	18.3	79.7
Specification AK1 TD.9	min. 700	850–1000	min. 14	min. 40
Specification WEV 400	min. 950	1000–1100	min. 12	min. 45

Table 4: Charpy impact test and hardness [HBW]
Tabela 4: Charpyjeva žilavost in trdota

Temperature, *T*/°C		+ 20 °C					Average value HBW 2.5/187.5
Blade No.	Sample	*KV*/J			*KCV*/(J/cm^3)	Required *R*/(J/cm^3)	
152	1PO-2PN-3PN	27	28	28	35	50	255
156	1PO-2PO-3PN	41	28	27	40		255
106	1PO-2PO-3PN	36	31	32	41		264
344	1PO-2PO-3PN	206	201	196	251		295

greatly influenced the propagation of the fatigue cracks (see **Figure 5**).

The microstructure of the base steel of X2CrNiMo13-4 consisted of sorbite, and was typical for the heat-treated (quenched and annealed) steel. No δ-ferrite inserts were found within the structure, even at a magnification of 400 (see **Figure 6**). The quantitative analysis of the amount of δ-ferrite is shown in **Figure 7**. The size of the original austenitic grains was evaluated according to the standards ČSN ISO 643 and ASTM E 112. A combination of Nital 3 % and Vilella-Bain etching agents was used to highlight the original austenitic grains. The obtained values showed that its size varied between 4.5 and 5.5 for both steel types (modified 12 % Cr martensitic steel and X2CrNiMo13-4 steel).

3.3 TEM

Figure 9 shows a grain of δ-ferrite in the modified 12 % Cr martensitic steel (**Figure 8**). The TEM revealed that the microstructure of blade No. 106 was similar to the microstructures of blades No. 152 and 156. Accord-

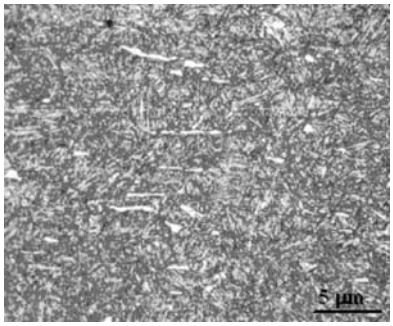

Figure 4: Blade No. 152 (PN), 200x, microstructure of base steel
Slika 4: Lopatica št. 152 (PN), mikrostruktura osnovnega jekla (200-kratna povečava)

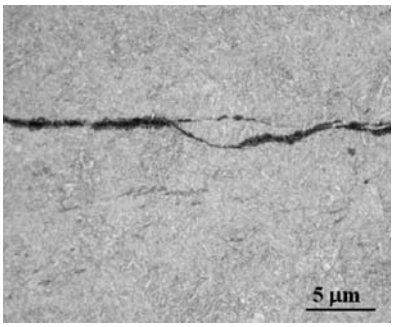

Figure 5: Blade No. 106, 200x, longitudinal crack and aligned inserts of δ-ferrite
Slika 5: Lopatica št. 106, podolžna razpoka in usmerjeni vložki δ-ferita (200-kratna povečava)

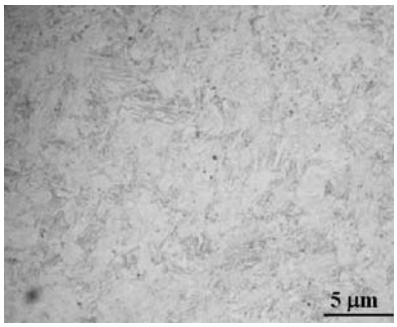

Figure 6: Blade No. 344 (PO), 200x, microstructure of base steel
Slika 6: Lopatica št. 344 (PO), mikrostruktura osnovnega jekla (200-kratna povečava)

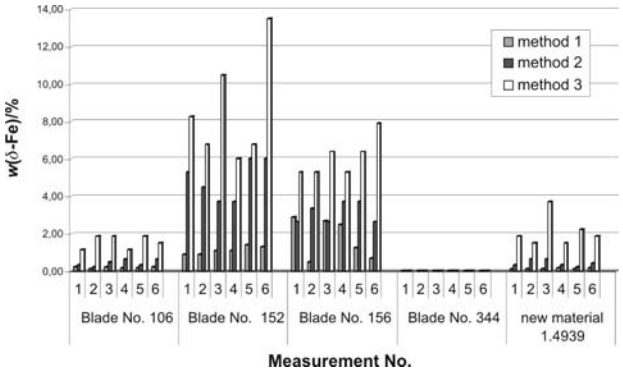

Figure 7: Content of δ-ferrite for different materials determined with different methods
Slika 7: Vsebnost δ-ferita v različnih jeklih, določena z različnimi metodami

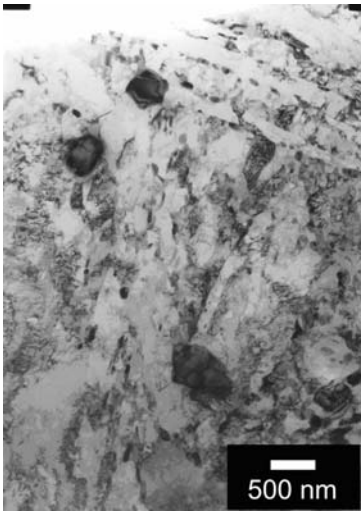

Figure 8: Blade No. 152, martensitic microstructure of base steel
Slika 8: Lopatica št. 152, martenzitna mikrostruktura osnovnega jekla

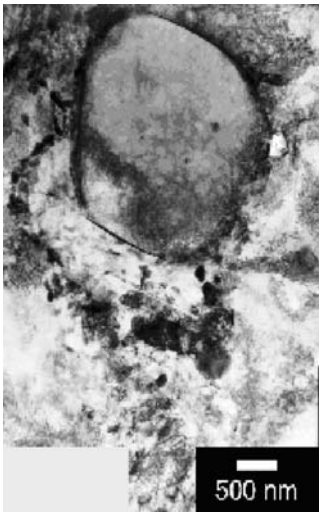

Figure 9: Blade No. 152, detail of δ-ferrite particle
Slika 9: Lopatica št. 152, detajl delca δ-ferita

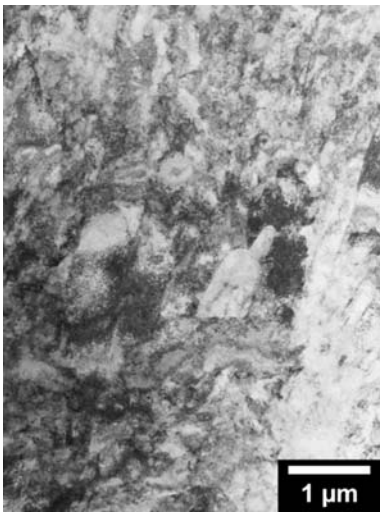

Figure 10: Blade No. 344, martensitic microstructure
Slika 10: Lopatica št. 344, martenzitna mikrostruktura

Figure 11: Blade No. 344, fine precipitates displayed in dark field
Slika 11: Lopatica št. 344, izločki, prikazani v temnem polju

ing to the electron diffraction results, the carbide particles were of the $M_{23}C_6$ type and the microstructure was practically without δ-ferrite.

Blade No. 344 of the steel X2CrNiMo13-4 (**Figure 10**) contained very fine precipitates of the intermetallic phase Fe_2Mo (**Figure 11**). Similar fine particles were also found in the newly developed steel 1.4939, which was free of coarser particles typical for the other analysed steel. Nevertheless, the local occurrence of a very limited quantity of these carbide particles cannot be excluded.

3.4 Fractographical analysis of damaged blades (modified 12 % Cr martensitic steel)

The fracture surfaces were covered with a thick layer of corrosion products that complicated the investigation of the micromorphology in the region of the fatigue cracks. These layers were removed with ultrasonic cleaning. The fractographical analysis showed that the cause of the blade damage was high-cycle fatigue-crack growth in the vicinity of the connection part of the blades and the gas-turbine shaft.

The cracks started on the blade surfaces in the upper groove of the connection area (see **Figure 12**) and then propagated with transcrystalline decohesion. It can be assumed that the δ-ferrite particles acted as the initiation points of the fracture. Many progressing lines were detected on the fracture areas of the damaged blades. The presence of these lines indicates that the loading was not constant and this is typical for fatigue fracture. From the number of progressing lines, the number of starting regimes of the gas turbine could be estimated.

From the width of certain growth rings it can be concluded that during stable operating conditions the crack-propagation stopped. From the microfractography it can be further concluded that the fatigue failure propagated with the striation mechanism (see **Figure 13a**).

Figure 12: Fracture area of blade No. 152 (the white arrow shows the front line beneath the striking edge)
Slika 12: Prelomna površina lopatice št. 152 (svetla puščica kaže na čelno črto pod udarnim robom)

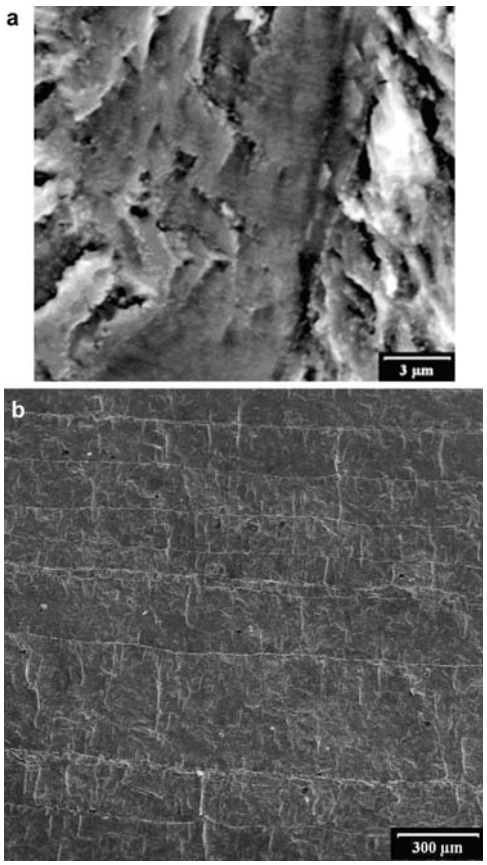

Figure 13: Characteristic microfractographical signs of fatigue failure. (a) Blade No. 152, field of submicron striations, (b) Blade No. 152, propagation lines
Slika 13: Karakteristični mikrofraktografski znaki utrujenostnega preloma. (a) Lopatica št. 152, področje submikrometrskih brazd, (b) lopatica št. 152, brazde propagacije

In addition, the presence of the progressing line determined the location and the shape of the fatigue crack tip at the moment of the overloading cycle. The dependence between these lines and the operating conditions made it possible to reconstruct the whole history of the failure process (see **Figure 13b**).

Estimation of the time-dependent failure propagation (modified 12 % Cr martensitic steel)

On the blades from the 3.TW (modified 12 % Cr martensitic steel AK1 TD. 9) on LP3 extensive maps were prepared (at various magnifications up to 300-times). This made it possible to obtain detailed information about the history of the fatigue-crack propagation.

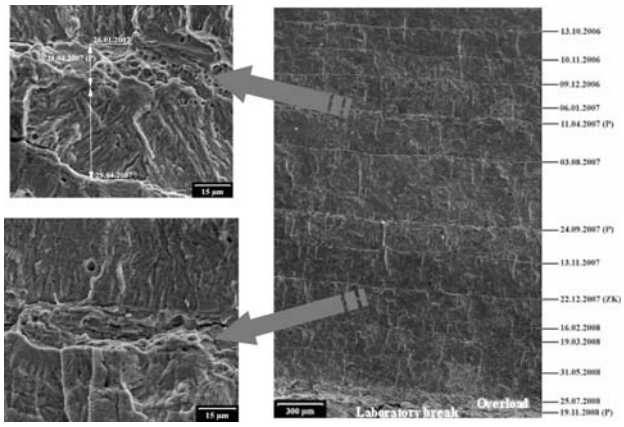

Figure 14: Blade No. 156. Propagation lines on the fracture area and dates of turbine operation

Slika 14: Lopatica št. 156. Linije propagacije razpoke in datumi rasti razpoke

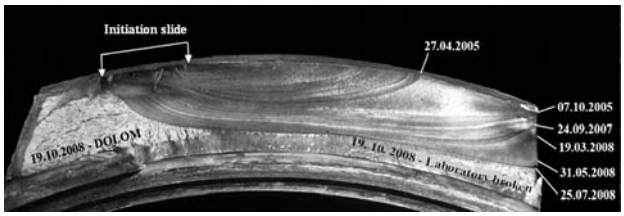

Figure 15: Blade No. 156. Dates, when the crack front reached the line of final blade failure

Slika 15: Lopatica št. 156. Na makrografiji je označen datum, ko je čelo razpoke doseglo mejo končnega preloma lopatice

The maps were closely analyzed with respect to the operation history of the gas turbine.

Figure 14 shows the propagation lines identified by these observations. These lines correspond to the data on the left-hand side of the micrograph. As mentioned above, the lines are related to the table operation of the turbine, and from the known data of the specific factory test the propagation regime on the fracture can be derived. The main results of the fatigue fraction history of the blades from 3.TW on LP3 in the fracture area can be seen in **Figure 15**.

4 CONCLUSION

The mechanical properties confirm that the requirements for the mechanical properties of most of the blades from the modified 12% Cr martensitic steel are fulfilled. However, the following exceptions were identified:

1. The blade No. 344 (X2CrNiMo13-4 steel) does not fulfil the requirements for ultimate strength. The lower value of 1.5 % is negligible, but it also positively affects the increase in the ductility parameters A_5 and Z.
2. The Charpy impact tests of blades No. 152, 156 and 106 revealed that measured values do not fulfil the requirement for impact toughness.
3. In contrast to the impact toughness of blade No. 344 (X2CrNiMo13-4 steel) was 2.5 times higher than required.
4. The hardness values fell within the required interval that allows higher hardness values within the blade No 344 (X2CrNiMo13-4 steel) in comparison with the modified 12 % Cr martensitic steel.

The low resistance to fatigue failures (mainly the resistance to fatigue-crack propagation) of the used materials in the working conditions can be stated as the main reason for the fatigue cracks' initiation.

The initiation of the fatigue cracks was a result of the presence of δ-ferrite (modified 12 % Cr martensitic steel). The fractographical reconstruction revealed that the initiation of the fatigue cracks in the blades started quite early after the initialization of the working process.

From the microstructural analysis it was concluded that the presence of δ-ferrite (the shape and the particles) negatively influences the resistance of the modified 12 % Cr martensitic steel to crack initiation. The subsequent propagation of fatigue cracks is controlled by the main operating load. The new material, 1.4939, without tungsten, which eliminates the presence of δ-ferrite to a large extent, is proposed for the manufacture of 3.TW blades.

5 REFERENCES

[1] J. Janovec, J. Siegl, CTU in Prague, 12/2008, Research report No. 10-08 Příčiny porušení lopatek 3. oběžných kol NT3 a NT1 TG1 ETE na 1. HVB (část 1) – (Causes of failure of 3th low pressure turbine wheel in LP3 and LP1 of TG1 in 1. HVB (part 1))

[2] J. Siegl, CTU in Prague, FJFI V-KMAT-746/08 – Research report Fraktografická analýza porušených lopatek NT dílů TG1 ETE (část 2) – (Fractographical analysis of failure blades LP parts of TG1 ETE (part 2))

[3] J. Siegl, CTU in Prague, FJFI V-KMAT/2009 Presentation Fraktografická analýza porušených loptek NT2 dílu TG2 ETE (Fractographical analysis of failure blades in LP2 parts of TG2 ETE))

[4] J. Janovec, J. Siegl, CTU in Prague, 12/2008 Presentation Příčiny porušení lopatek 3. oběžných kol NT3 a NT1 TG1 ETE na 1. HVB (Causes of failure 3rd in LP3 and LP1 of TG1 ETE)

[5] J. Zenkl, O. Novák, ČEZ, a.s. ETE, ČEZ, a.s. EDU, Analýza příčin poškození lopatek na NT dílech TG 1000 MW (Analysis of the causes of damage to the blades on LP parts TG 1000 MW)